Upper Limb Cortical-Muscular Coupling Analysis Based on Time-Delayed Back Maximum Information Coefficient Model

Qingshan She, Guomei Jin, Renfei Zhu, Michael Houston, Ouguan Xu, and Yingchun Zhang, *Senior Member, IEEE*

***Abstract*— In musculoskeletal systems, describing accurately the coupling direction and intensity between physiological electrical signals is crucial. The maximum information coefficient (MIC) can effectively quantify the coupling strength, especially for short time series. However, it cannot identify the direction of information transmission. This paper proposes an effective time-delayed back maximum information coefficient (TDBackMIC) analysis method by introducing a time delay parameter to measure the causal coupling. Firstly, the effectiveness of TDBackMIC is verified on simulations, and then it is applied to the analysis of functional cortical-muscular coupling and intermuscular coupling networks to explore the difference of coupling characteristics under different grip force intensities. Experimental results show that functional cortical-muscular coupling and intermuscular coupling are bidirectional. The average coupling strength of EEG→EMG and EMG→EEG in beta band is 0.86 ± 0.04 and 0.81 ± 0.05 at 10% maximum voluntary contraction (MVC) condition, 0.83 ± 0.05 and 0.76 ± 0.04 at 20% MVC, and 0.76 ± 0.03 and 0.73 ± 0.04 at 30% MVC. With the increase of grip strength, the strength of functional cortical-muscular coupling in beta frequency band decreases, the intermuscular coupling network exhibits enhanced connectivity, and the information exchange is closer. The results demonstrate that TDBackMIC can accurately judge the causal coupling relationship, and functional cortical-muscular coupling and intermuscular coupling network under different grip forces are different, which provides a certain theoretical basis for sports rehabilitation.**

***Index Terms*— EEG signal, EMG signal, intermuscular coupling network, functional cortical-muscular coupling, information flow.**

Manuscript received 3 July 2023; revised 14 October 2023; accepted 10 November 2023. Date of publication 20 November 2023; date of current version 30 November 2023. This work was supported in part by the Zhejiang Provincial Natural Science Foundation of China under Grant LZ22F010003, in part by the National Natural Science Foundation of China under Grant 62371172, and in part by the Joint Funds of the Zhejiang Provincial Natural Science Foundation of China under Grant LZJWZ23E090001. *(Corresponding authors: Ouguan Xu; Yingchun Zhang.)*

This work involved human subjects or animals in its research. Approval of all ethical and experimental procedures and protocols was granted by the Ethics Committee of Dongyang People's Hospital under Application No. 2022-YX-253.

Qingshan She, Guomei Jin, and Renfei Zhu are with the School of Automation, Hangzhou Dianzi University, Hangzhou, Zhejiang 310018, China, and also with the International Joint Research Laboratory for Autonomous Robotic Systems, Hangzhou, Zhejiang 310018, China.

Michael Houston and Yingchun Zhang are with the Department of Biomedical Engineering, University of Houston, Houston, TX 77204 USA (e-mail: yingchun.umn@gmail.com).

Ouguan Xu is with the College of Information Engineering, Zhejiang University of Water Resources and Electric Power, Hangzhou, Zhejiang 310018, China (e-mail: xuog@zjweu.edu.cn).

Digital Object Identifier 10.1109/TNSRE.2023.3334767

I. Introduction

IN THE process of human autonomous movement, the motor cortex sends control information to the effector muscle through the motor nerve pathway, and the muscle feedbacks the information to the motor cortex, forming a closed loop. Functional cortical-muscular coupling (FCMC) is the interaction or coherence between the cerebral motor cortex and muscle tissue. It indicates how the cortex performs actions, and the deeper meaning lies in the mode of information processing and motion generation [1]. FCMC is believed to be the key to direct or indirect signal transmission between the motor cortex and the effector muscles [2]. In 1995, Conway et al. [3] proposed the first FCMC coherence study based on the synchronous oscillation relationship between EEG and EMG sequences. In later studies [4], [5], FCMC, as a neurophysiological measure, has been widely used in the assessment of rehabilitation after disease, especially stroke. The concept of intermuscular coupling (IMC) is similar to FCMC. It refers to the mutual connection between muscles with different functions under the same action, which reflects the corticospinal drive shared by the motor neurons of related muscles [6]. In recent years, many studies have collected electroencephalogram (EEG) signals and surface electromyogram (EMG) signals to explore the pathological mechanism of motor dysfunction through the analysis of functional cortical-muscular coupling and intermuscular coupling, which evaluate the rehabilitation effect of patients with neurological diseases such as stroke [7], [8], [9].

The relationship between neurophysiological electrical signals mainly includes two aspects: coupling strength and coupling direction. At present, the algorithms for quantifying the functional cortical-muscular coupling and intermuscular coupling mainly include coherence [10], mutual information (MI) [11], Granger causality (GC) [12], and transfer entropy (TE) [13]. The coherence and mutual information methods are both based on the assumption of symmetry in the relationships between variables, which hinders their ability to

accurately identify the direction of information propagation, limiting their practical applications. GC and TE can not only quantify the coupling strength, but also identify the coupling direction, and they meet the needs of detecting the relationship between neurophysiological electrical signals. However, the neurophysiological electrical signals have been proved to be nonlinear [14]. The GC method is based on a linear system [15]. The TE method used to detect nonlinear systems is an extension of GC. Specially, for the linear Gaussian model, TE is equivalent to GC. Therefore, TE is the most effective method to detect the causal relationship of the neurophysiological electrical signals, it is also widely used in other fields [16], [17]. However, in practical applications, when the time series is not long enough, TE cannot accurately detect the coupling relationship [18].

Reshef et al. [19] proposed the maximum information coefficient (MIC) method to calculate the linear and nonlinear correlation of two variables. MIC can capture the broad correlation (i.e., universality) between different functions, and has the same correlation metric (i.e., fairness) for any function with the same noise. In recent years, MIC has been applied to the field of neuroscience. Tian et al. [20] used MIC as a supplementary method for PCC to reveal the mechanism of brain network in resting state. Liang et al. [21] extended MIC to the time-frequency domain to study the cortical-muscular function coupling in flexion of back muscles. However, for the relationship between two variables, MIC is represented by a scatter plot, two sets of data form multiple coordinate points, which distribute in two-dimensional space. The two-dimensional space is divided into different grids along the horizontal and vertical axes, and find the grid scheme that maximizes mutual information, and its calculation is very intensive. Therefore, there have been many studies on the optimization of MIC algorithm. Reshef et al. [19] used the algorithm ApproxMaxMI to calculate MIC. However, the averaging strategy adopted by the algorithm to quickly obtain the optimal grid is not a necessary condition to obtain MIC, and the universality of MIC is closely related to the maximum grid limit. Zhang et al. [22] used simulated annealing and genetic algorithm to optimize MIC. This algorithm can obtain better MIC values, but it is more time-consuming. Chen et al. [23] proposed ChiMIC algorithm for this problem, this algorithm used the χ^2 test to control the number of segments in the optimization direction, but its non-optimization direction still adopts the averaging strategy and failed to achieve bidirectional unequal spacing grid division. Cao et al. [24] proposed a MIC optimization algorithm BackMIC which is based on ChiMIC, and this algorithm adds the backtracking optimization process to eliminate the limit of averaging. However, BackMIC is symmetrical and cannot distinguish the direction between signals.

To solve the limitation of the BackMIC method in the direction of information transmission, inspired by the idea of TDMI [18] and TDMIC [25], this paper introduces a time delay parameter into BackMIC and proposes the timedelayed back maximum information coefficient (TDBackMIC) algorithm, which infers the causal relationship by capturing the information transmission delay between two time series. First, the steps of this method are briefly introduced. Then, the effectiveness of the method is verified by simulation. Finally, the algorithm is applied to the study of functional corticomuscular coupling and intermuscular coupling network under different grip forces, and the differences of coupling characteristics under different grip forces is discussed in depth, which can provide a new method for exploring the diagnosis and rehabilitation of neuromuscular diseases.

The main contributions of this paper are summarized as follows:

1) We propose a TDBackMIC method to accurately determine the causal relationship between variables. This method has strong robustness to variables.

2) The calculation steps of the causal judgment algorithm are described in detail. The effectiveness of TDBackMIC algorithm is verified by simulation experiments.

3) TDBackMIC algorithm was applied to the analysis of functional cortical-muscular and intermuscular coupling networks, demonstrating the differences in coupling characteristics under different grip strength.

II. Proposed Method

A. MIC

The MIC algorithm can measure the linear and nonlinear correlation between two random variables. The MIC of random variables X and Y is defined as follows:

$$MIC(X,Y) = \max_{n_x \times n_y \le B(n)} \left\{ \frac{MI^*_D(X,Y)}{\log_2 \min(n_x, n_y)} \right\}. \quad (1)$$

where n_x and n_y (positive integer) are the number of grids on the x-axis and y-axis respectively, D represents the $n_x \times n_y$ grid, $MI^*_D(X,Y)$ is the maximum mutual information among all grid division methods under a fixed number of grids, $\log_2 \min(n_x, n_y)$ normalizes mutual information. $B(n) = n^\alpha$ is a function that upper bounds the number of grids, n is the size of data, and α $(0 < \alpha < 1)$ is a constant. Choosing the appropriate size of $B(n)$ is important, which is usually set to $B(n) = n^{0.6}$ $(\alpha = 0.6)$ by default. The value of $MIC(X,Y)$ is between [0,1]. The larger the value is, the stronger the coupling between the two variables is, and vice versa.

B. TDBackMIC Algorithm

The principle of MIC algorithm is to find the grid division method when the mutual information is the largest from two grids of different dimensions. Finding the optimal grid division is computationally expensive. BackMIC uses the χ^2 test to terminate the grid search. The calculation description of the χ^2 statistic is shown in **Fig. 1**. The vertical axis is divided into r segments, and the new segmentation point P_k on the horizontal axis is between P_{k-1} and P_{k-2}, the $c-1$ and c columns are divided. The yellow area in the figure is defined as the detection area of the segmentation point P_k for χ^2 test. The χ^2 statistic is defined as:

$$\chi^2_{P_k} = \sum_{j=1}^{r} \sum_{i=c-1}^{c} \frac{(n_{j,i} - n_{*,i} n_{j,*}/N)^2}{n_{*,i} n_{j,*}/N}. \quad (2)$$

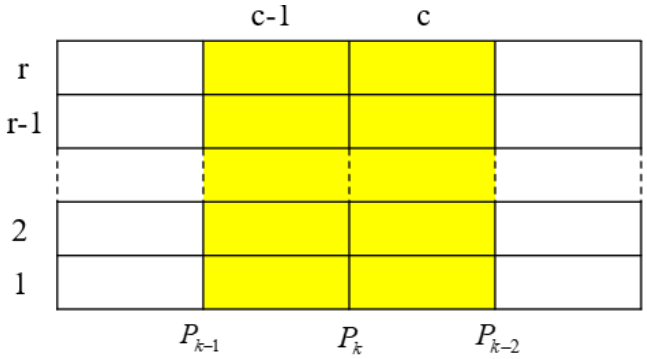

Fig. 1. The calculation description of the χ^2 statistic. The yellow area is the detection area of the segmentation point P_k for χ^2 test.

where N is the number of data points in the detection area, $n_{*,i}$ is the number of data points in the column i, $n_{j,*}$ is the number of data points in the detection area in the row j, and $n_{j,i}$ is the number of data points in the row j and column i. BackMIC uses the χ^2 test for the new segmentation point. If the value is greater than the preset threshold, which indicates that the segmentation point is valid, the search for the next segmentation point is continued and the χ^2 test is used. Otherwise, the search for the axis segmentation point is paused.

When searching the optimal grid, the BackMIC algorithm first divides the vertical axis equally into r segments ($r = 2, 3, \ldots, B(n)/2$), obtains the optimal segmentation point on the horizontal axis through the χ^2 test, and fixes it on the horizontal axis, and then obtains the optimal segmentation point on the vertical axis through the χ^2 test. BackMIC algorithm obtains the bidirectional unequal interval grid division, and then calculates the corresponding normalized mutual information under the grid division.

Because BackMIC is symmetric, the algorithm cannot recognize the coupling direction. To solve this problem, we refer to the TDMIC algorithm, introduce a delay parameter and propose the TDBackMIC algorithm. The direction of the information flow is determined by calculating the BackMIC between the variable X and the variable Y with different delays $\tau(BackMIC(X, Y, \tau))$. When $BackMIC(X, Y, \tau)$ reaches peak value, the corresponding τ value is negative which represents $X \rightarrow Y$, the corresponding τ value is positive which represents $Y \rightarrow X$. In order to estimate the total information flow intensity over a period of time, the following formula can be used to calculate the cumulative information flow within a specific delay Q:

$$C_{TDBackMIC} = \sum_{i=1}^{Q} TDBackMIC(k, i). \tag{3}$$

Here, the delay Q is set to 40 data points and k is set to 1.

C. Establishment of Intermuscular Coupling Network

The intermuscular coupling network is essentially a directed weighted complex network. $V = \{v_1, v_2, \ldots, v_m\}$ is a collection of muscle nodes, $v_i \in V, (i = 1, 2, \ldots, m)$ is a node in the network, m is the number of nodes in the intermuscular coupling network, and $v_i \rightarrow v_j$ represents a directed edge from node v_i to node v_j. $TDBackMIC_{v_i \rightarrow v_j}$ indicates the connection weight on the directed edge $v_i \rightarrow v_j$. Generally, $TDBackMIC_{v_i \rightarrow v_j}$ and $TDBackMIC_{v_j \rightarrow v_i}$ are not equal.

The network construction needs to be thresholded. If the threshold is too small, the intermuscular coupling network contains false connections, which will cover up important topological relationships. If the threshold is too large, the intermuscular coupling network is too sparse and loses a lot of meaningful information. In this paper, according to the threshold selection [26], the threshold is set between $0.05 \sim 0.95$ *max($TDBackMIC$), which is reduced by 0.05 *max($TDBackMIC$) until there is no isolated node, where max($TDBackMIC$) is the maximum value in the network. The adjacency matrix of intermuscular coupling network is D, and the threshold value is h, then the adjacency matrix A after thresholding is

$$A_{ij} = \begin{cases} D_{ij}, & D_{ij} \geq h \\ 0, & D_{ij} \geq h. \end{cases} \tag{4}$$

D. Parameters of Intermuscular Coupling Network

In this paper, node strength and clustering coefficient [27] are used to analyze the characteristics of intermuscular coupling network in different frequency bands under different grip forces from the overall perspective.

1) Node Strength: The node strength in a directed network can be divided into entry degree and exit degree. The higher the node strength is, the more important the node is in the network. The entry degree and exit degree of each node v_i are $H_{in}(v_i)$ and $H_{out}(v_i)$ respectively. The larger the value of $H_{in}(v_i)$ is, it indicates that there are more nodes that can affect this node. The larger the value of $H_{out}(v_i)$ is, the greater the contribution of this node is, the more important its position in the network is. The average degree of intermuscular coupling network HN is defined as

$$HN = \frac{1}{2 \times m} \sum_{i=1}^{m} (H_{in}(v_i) + H_{out}(v_i)). \tag{5}$$

The higher the average degree of the network is, the stronger the correlation between the channels is.

2) Clustering Coefficient: The clustering coefficient of node $C(v_i)$ measures the degree of network community structure. The larger the node clustering coefficient is, the higher the degree of interconnection between this node and other nodes. The clustering coefficient of intermuscular coupling network CN is defined as

$$CN = \frac{1}{m} \sum_{i=1}^{m} C(v_i). \tag{6}$$

Here, $CN \in [0, 1]$. When $CN = 0$, it means that all nodes in the network are isolated nodes. When $CN = 1$, it means that every node in the network is fully connected to others.

III. Experimental Data Acquisition and Preprocessing

A. Data Acquisition

The data was collected from 10 healthy adults (21∼25 years old). All subjects were right-handed, and had no upper

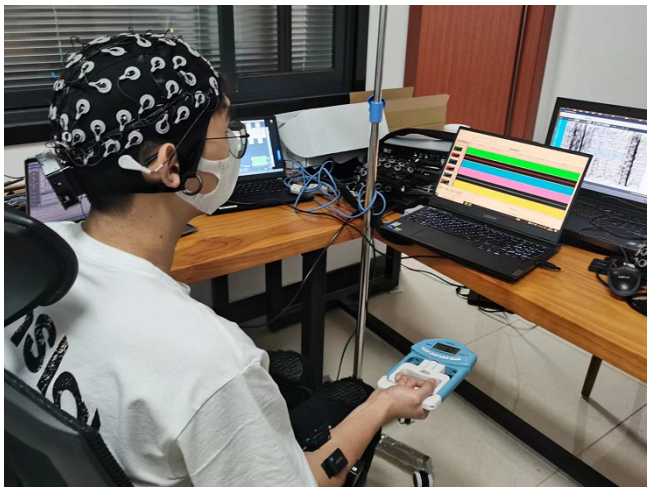

(a) Experimental environment of upper limb grasping

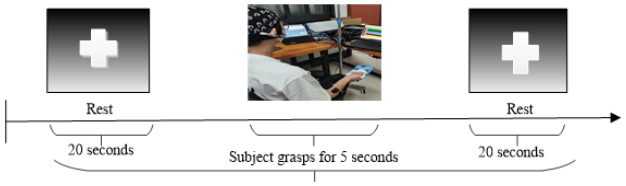

(b) Experimental flow chart. One trial lasted 25 seconds, including 5s of grip test and 20s of post-rest time.

Fig. 2. Experimental setup.

limb motor dysfunction or history of joint injury. All the subjects were in good mental condition, were informed of the details of the experiment, signed the informed consent form and volunteered to participate in the data collection experiment. The EEG signals and the EMG signals of right hand, including brachioradialis (B), biceps brachii (BB), flexor carpi ulnaris (FCU), flexor digitorum superficialis (FDS), flexor carpi radialis (FCR) and extensor digitorum (ED) were collected synchronously. Before the experiment, the skin of the collection site was cleaned with 75% medical alcohol. The maximum voluntary contraction (MVC) of each subject was then tested. Sensors were placed on the muscles corresponding to the movement according to the anatomical knowledge. The upper limb grasping experimental environment is shown in **Fig.** 2(a). The subjects' grasping action continued to sample for 5 seconds, and then rested for 20 seconds. The sampling frequency was 1000Hz. Each subject carried out three experiments, and the subjects completed 10%, 20%, and 30% MVC grasp respectively. The whole experimental process is shown in **Fig.** 2(b). Based on preliminary data reported in previous studies [25], [28] that reported corticomuscular coupling under varying MVC levels, we estimated that ten subjects would be sufficient for the intended analysis.

B. Data Preprocessing

EMG signals underwent a 50Hz notch filter and a 0.5∼200Hz bandpass filter. EEG signals underwent a 50Hz notch filter and a 0.5∼75Hz bandpass filter. The Chebyshev II bandpass filter was then used to extract the EEG and EMG signals in the beta band (15Hz∼30Hz) and gamma band (31Hz∼60Hz) for further analysis.

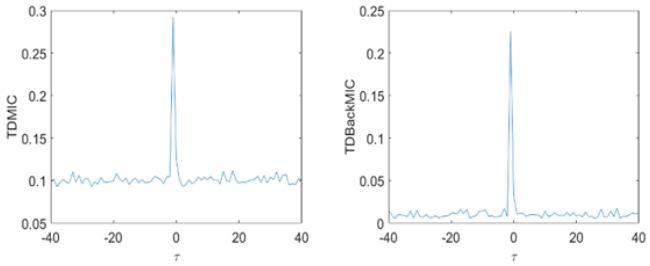

(a) (b)

Fig. 3. Comparison between TDMIC and TDBackMIC (Model 1). (a) shows the TDMIC curve of the time series X and Y generated by Model 1. (b) shows the TDBackMIC curve of the time series X and Y generated by Model 1.

IV. Simulations

To verify the effectiveness of the TDBackMIC method, the following three simulation models are constructed for test and analysis.

A. Model 1

A directed linear system, there is information flow from time series X to Y.

$$\begin{cases} x_t = -0.3x_{t-1} + \varepsilon_t \\ y_t = 0.3y_{t-1} - 0.9x_{t-1} + \eta_t. \end{cases} \tag{7}$$

where ε_t and η_t are Gaussian noises with mean value of 0 and variance of 1, the same below.

B. Model 2

A directed nonlinear system, there is information flow from time series X to time series Y.

$$\begin{cases} x_t = 0.6x_{t-1} + \varepsilon_t \\ y_t = 0.6y_{t-1} + 0.5x_{t-1}^2 + \eta_t. \end{cases} \tag{8}$$

C. Model 3

A directed nonlinear system, compared with Model 2, the relationship between time series X and Y is more complex, and there is information flow from time series X to time series Y.

$$\begin{cases} x_t = 0.4x_{t-1} + \varepsilon_t \\ y_t = 1.5 * [2x_{t-1} + \cos^2(x_{t-1})] + \eta_t. \end{cases} \tag{9}$$

The above three models use TDMIC and TDBackMIC methods respectively for analysis and comparison.

Model 1 and Model 2 are randomly generated for 10 times. **Fig.** 3 and **Fig.** 4 show the comparison of the TDMIC and TDBackMIC curves of the time series X and Y generated by Model 1 and Model 2. The value of α is set to 0.6 to limit the number of grids searched. It can be seen that whether a linear system or a nonlinear system, both TDMIC and TDBackMIC reach a significant peak when the time delay is negative, which indicates that the identified information flow direction is X to Y, this is consistent with the predetermined direction of the model. TDMIC and TDBackMIC can accurately judge the direction of the 10 times time series randomly generated by Model 1 and Model 2, which shows that both methods can

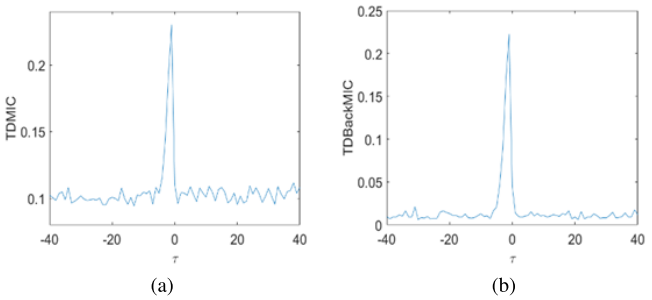

Fig. 4. Comparison between TDMIC and TDBackMIC (Model 2). (a) shows the TDMIC curve of the time series X and Y generated by Model 2. (b) shows the TDBackMIC curve of the time series X and Y generated by Model 2.

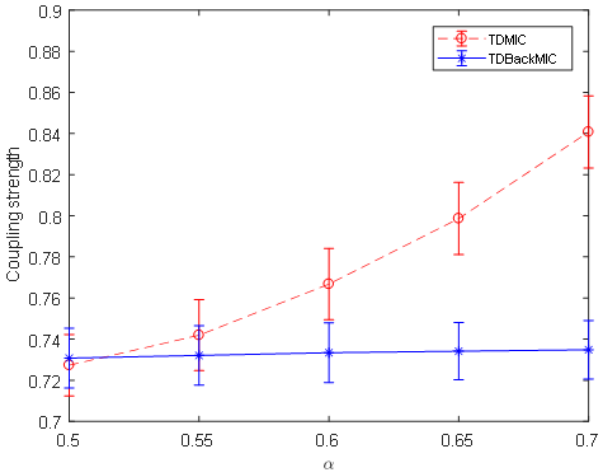

Fig. 5. Comparison of TDMIC and TDBackMIC of time series X to Y under different α.

accurately identify the direction of information flow of linear and nonlinear systems.

Fig. 5 shows the comparison of TDMIC and TDBackMIC of the time series X and Y randomly generated by Model 3 for 10 times in different α. TDMIC increases with the value of α increases, while TDBackMIC remains almost unchanged. Therefore, the TDBackMIC method is more robust than TDMIC in terms of variable α, which further proves that the TDBackMIC proposed in this paper is an excellent measure of causal coupling.

V. Experimental Results

This paper analyzes the characteristics of functional cortical-muscular coupling and intermuscular coupling network in different frequency bands and different grip strength levels in the upper limb grasping experiment. It provides a good basis for evaluating the grip strength and the rehabilitation of stroke patients.

A. Cortical-Muscular Function Coupling

In this paper, the EEG signal of C3 channel in the motor cortex and the EMG signal of FDS are selected for the functional cortical-muscular coupling analysis. The bidirectional coupling intensity of EEG and EMG was calculated using

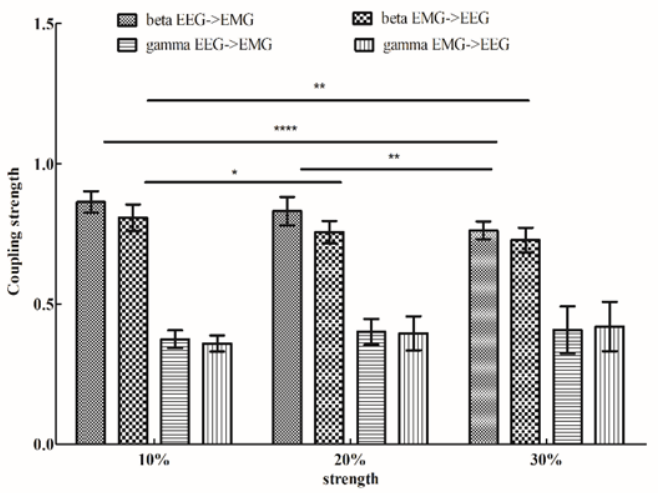

Fig. 6. Cortical-muscular coupling strength between different frequency bands under different forces. The significance level is 0.05, where '*' represents $p<0.05$, '* *' represents $p<0.01$, '* * *' represents $p<0.001$, and '* * * *' represents $p<0.0001$.

the TDBackMIC algorithm. **Fig. 6** shows the mean value and standard deviation of functional cortical-muscular coupling strength in different frequency bands under different grip strength levels of all subjects. Independent sample T test is conducted for the coupling strength of each frequency band under different grip strength levels. It can be seen from **Fig. 6** that regardless of the grip strength, the coupling strength of $EEG \rightarrow EMG$ and $EMG \rightarrow EEG$ of the beta frequency band are significantly greater than that of the gamma frequency band, and the coupling strength of $EEG \rightarrow EMG$ on the beta frequency band is greater than that of $EMG \rightarrow EEG$, which indicates that the transmission of information from the cerebral motor cortex is dominant. With the increase of grip strength, the bidirectional coupling strength on the beta frequency band decreases significantly, while the coupling strength on the gamma frequency band has no significant difference.

B. Intermuscular Coupling Network

According to the coupling calculated by TDBackMIC, the thresholded adjacency matrices of all subjects in each frequency band are averaged, and the directed intermuscular coupling network is established and analyzed. Taking the average coupling strength of subjects at 30% MVC as an example, the muscle functional network diagrams of two main frequency bands (beta and gamma) are established. The direction of the arrow indicates the direction of information transmission. The thickness of the edge reflects the strength of intermuscular coupling. The thicker the line is, the greater the coupling strength between the two nodes connected by the line is. The size of a node represents the average value of its entry degree and exit degree. The larger the node is, the more important this node is in the network. It can be seen from **Fig. 7**, the information transmission between muscle nodes is bidirectional. **Table I** shows the entry degree of nodes, it can be seen that the entry degree of FCU, FDS, and FCR are relatively high, this indicates that the information flow mainly flows to FCU, FDS, and FCR. In both beta and

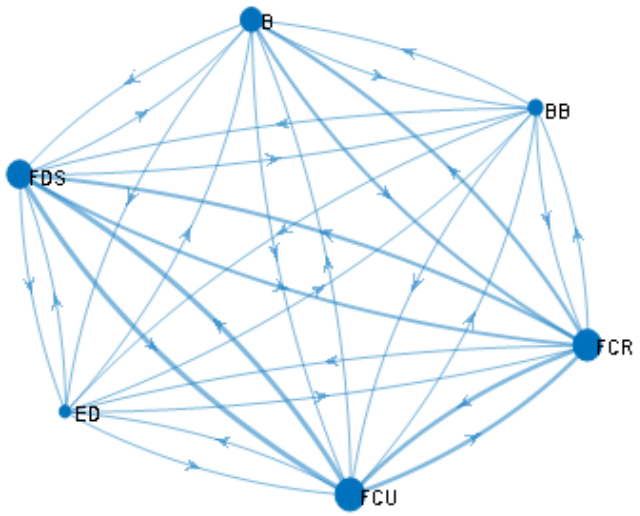

(a) beta band

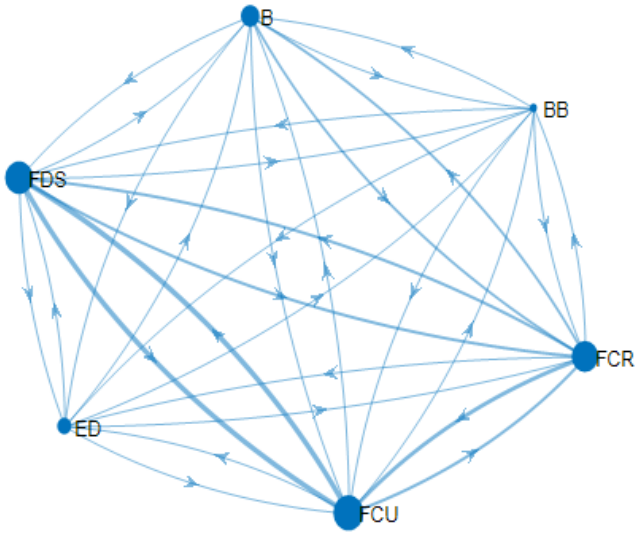

(b) gamma band

Fig. 7. Intermuscular coupling network of different frequency bands at 30% MVC. The direction of the arrow represents the direction of information transmission, the size of the node represents the average value of its entry degree and exit degree, and the line between the nodes represents the size of the coupling strength.

TABLE I
THE ENTRY DEGREE OF NODES IN INTERMUSCULAR COUPLING NETWORKS OF DIFFERENT FREQUENCY BANDS AT 30% MVC

	FCU	FDS	FCR	B	ED	BB
beta	0.0612	0.0539	0.0571	0.0443	0.0247	0.0309
gamma	0.0609	0.0544	0.0477	0.0322	0.0296	0.0115

gamma frequency bands, the coupling strength between FDS and FCU, between FCU and FCR, and between FDS and FCR is significantly greater than that between other muscle nodes. FDS, FCU and FCR have a greater degree of exit and entry. BB and ED have smaller exit degree and entry degree than other nodes. When the network threshold increases, they are more likely to become isolated nodes of the network. This shows that FDS, FCR and FCU cooperate with each other in

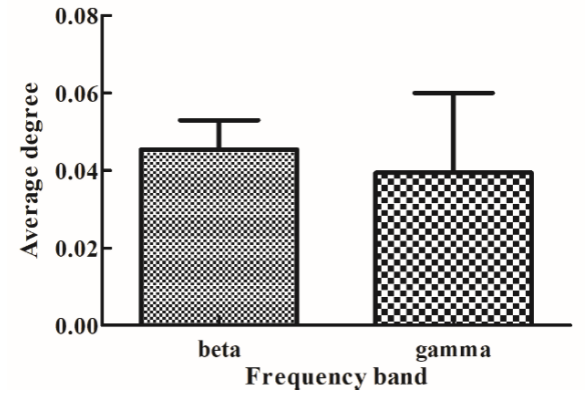

(a)

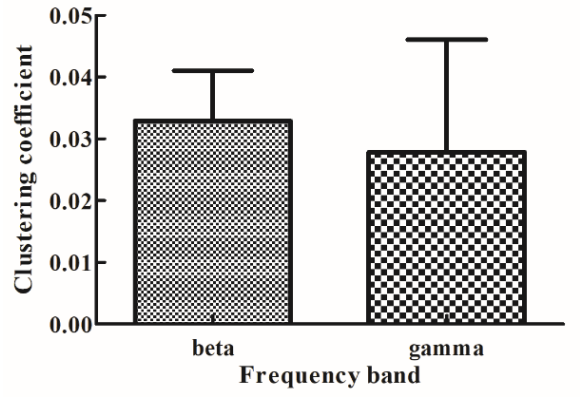

(b)

Fig. 8. Comparison of parameters of intermuscular coupling network in different frequency bands at 30% MVC.

grasping action, and play a leading role in network information interaction.

In order to better quantify the characteristics of the intermuscular coupling network, the average degree and clustering coefficient of the intermuscular coupling network in each frequency band were calculated, and the independent sample T tests were conducted. The comparison of the characteristic parameters of the muscle functional network is shown in Fig. 8. The result shows that the average degree and clustering coefficient in the beta frequency band are greater than those in the gamma frequency band and there is no significant difference.

Because the intermuscular coupling strength is greater in the beta frequency band [25], we analyze the differences of intermuscular coupling network in the beta frequency band under different grip forces. The intermuscular coupling network diagram of all subjects in beta frequency band under different grip forces is shown in Fig. 9. The entry degree of nodes in intermuscular coupling networks under different grip forces is shown in Table II. It can be seen from the figure and table that the entry degree of FCU, FDS, and FCR are relatively high, with the increase of grip force, the coupling strength between muscles slightly increases, and the degree of exit and entry of muscle node also increase, which indicates that for the completion of different grip forces movement, the contribution of muscles increases. At 10% MVC, there are mainly three muscles to maintain grip force, and BB has small

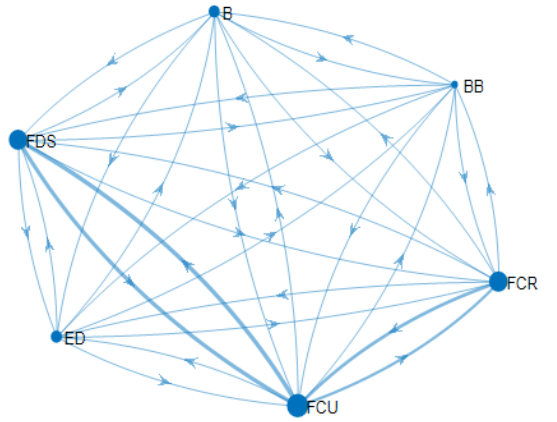

(a) 10% MVC

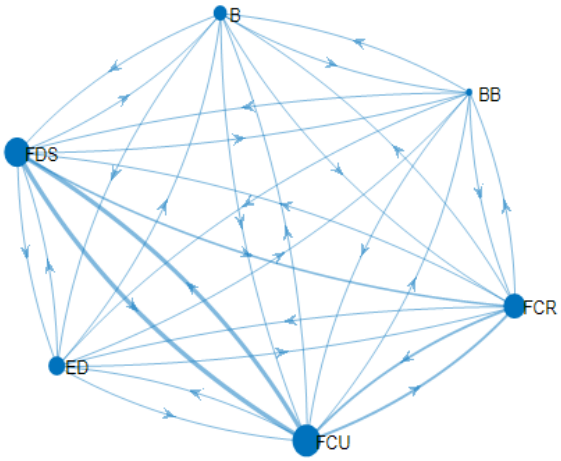

(b) 20% MVC

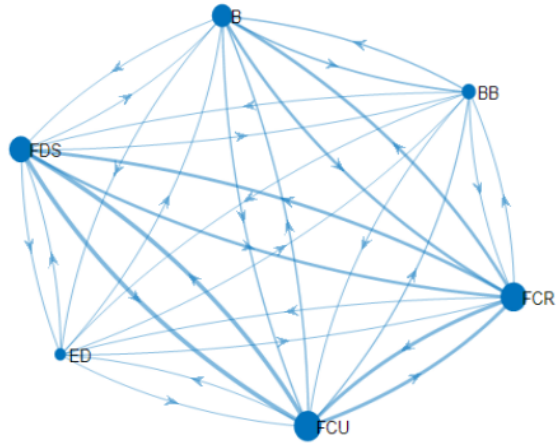

(c) 30% MVC

Fig. 9. Intermuscular coupling network under different grip forces.

exit degree and entry degree. At 20% MVC, the entry degree of FDS and ED increased greatly, while the entry degree of BB decreased. But at 30% MVC, more muscles participate in the action, and the information interaction between muscles increases, which is more conducive to maintain a higher grip strength level.

TABLE II
THE ENTRY DEGREE OF NODES IN INTERMUSCULAR COUPLING NETWORKS UNDER DIFFERENT GRIP FORCES

	FCU	FDS	FCR	B	ED	BB
10% MVC	0.0505	0.0422	0.0388	0.0204	0.0261	0.0136
20% MVC	0.0615	0.0555	0.0485	0.0278	0.0368	0.0126
30% MVC	0.0612	0.0539	0.0571	0.0443	0.0247	0.0309

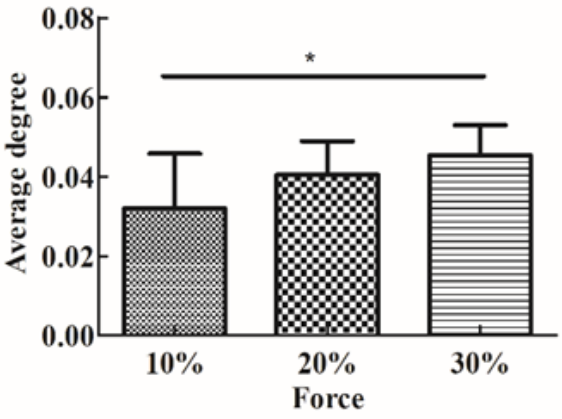

(a)

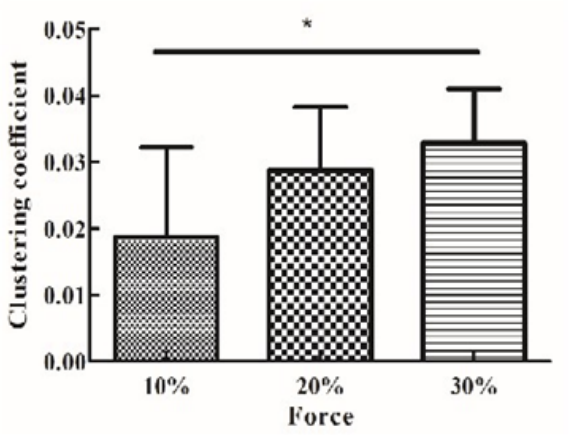

(b)

Fig. 10. Parameter comparisons of intermuscular coupling network under different grip forces. '*' Indicates that the p-value is less than 0.05.

In order to analyze the difference of intermuscular coupling network under different grip forces, we calculate two important parameters of network characteristic. The mean value and standard deviation of all subjects are calculated and shown in Fig. 10. The experimental result shows that in the beta frequency band, with the increase of grip force, the average degree and clustering coefficient also increase and there are significant differences. The intermuscular coupling network is different in different grip forces, which indicates that the central nervous system works in a specific way to cope with the changes in grip strength.

VI. DISCUSSION

In the process of human motion, the central nervous system transmits the motion control information to the relevant

muscles through neural oscillation, which causes the oscillation of the motor unit, and then reveals the interaction between the cerebral cortex and the muscle. Under the control of the central nervous system, the coupling relationship between muscles at different time and space levels reflects the interaction between related muscles in the process of exercise. In this paper, TDBackMIC method is proposed to analyze the characteristics of functional cortical-muscular coupling and intermuscular coupling network in different frequency bands of EEG and EMG signals under different grip forces.

Firstly, the proposed TDBackMIC method is simulated. The simulation result shows that TDBackMIC can effectively identify the direction of information flow, and TDBackMIC has stronger robustness on variable α than the previous TDMIC method. It provides a new causal measurable method for understanding the characteristics of complex functional cortical-muscular coupling and intermuscular coupling network.

When the subject grasps, the cerebral motor cortex transmits command information to the muscle, which reflects in the coupling direction $EEG \rightarrow EMG$. At the same time, the muscle also feedback the information to the cerebral cortex, which corresponds to the coupling direction $EMG \rightarrow EEG$, and the coupling strength of $EEG \rightarrow EMG$ in the beta frequency band is greater than $EMG \rightarrow EEG$, which fully indicates that the EEG and EMG are in the same closed loop, and their coupling is bidirectional. It is consistent with the existing research conclusions [29]. Liu et al. [30] points out that few studies have observed strong coupling in the low gamma band in stability-output tasks. The coupling of gamma bands in this study may be related to the setting and execution level of the motion plan. Fine force tracking tasks, which require high attention resources and require complex fusion of visual and somatosensory information [30], may also lead to this condition. Extensive studies have shown that [31], [32] the functional cortical-muscular coupling in beta frequency band is related to the output of steady-state force, and functional cortical-muscular coupling in gamma frequency band is related to the output of dynamic force. The coupling strength of beta frequency band is significantly greater than that of gamma frequency band during grip movement, which is consistent with the existing research [33]. With the increase of grip force, the coupling strength of beta frequency band decreases significantly, which may be because the subjects need to consume more energy to maintain the output of larger constant force, making the EEG and EMG coupling system in an unstable state. It is confirmed that the coupling in the beta frequency band reflects in the control function of the cortex to stable states [34].

The development of complex networks makes it possible to analyze the intermuscular motion mechanism from a holistic perspective. It can not only analyze the coupling between a pair of muscles, but also analyze the characteristics of the intermuscular coupling network from a global perspective. In order to deeply study the differences of the intermuscular coupling network of the subjects under different grip forces and different characteristic frequency bands, this paper divides the signals of the six EMG channels collected by the subjects at 10%, 20% and 30% MVC into two characteristic frequency bands, beta and gamma, and then uses TDBackMIC to calculate the intermuscular coupling strength and builds the intermuscular coupling network. The experimental result shows that FCU and FDS are the key muscles, and the coupling strength between FCU and FDS is larger under different grip forces and different frequency bands, FCU and FDS can be regarded as a pair of cooperative muscles of grip movement, which is consistent with the results obtained in existing study [25]. The intermuscular coupling is bidirectional, which is similar to the cortical-muscular function coupling. The stronger information flow mainly flows to the synergistic muscles (i.e., FDS, FCU, and FCR), this is consistent with the results obtained in existing study [25]. The correlation between muscles in beta frequency band is stronger, and the network connectivity is greater. This may be because the intermuscular coupling in beta frequency band has been proved to be related to the output of steady-state force [35]. In addition, with the increase of grip force, more muscles participate in the movement of constant grip force, and the information interaction between non-key muscle BB and other muscles increases, which reflects in the increase of the degree of exit and entry of BB node. The node degree and clustering coefficient also increase with the increase of grip force, which indicates that the greater the grip force is, the closer the information interaction is. To some extent, it reflects that the adjustment of the control strategy of the neural control system to cope with the output of greater and constant grip force. There are differences in the coupling strength between muscles, which may be related to the different functions of muscles. It reflects different motion control mechanisms, which is consistent with previous studies [36].

The proposed TDBackMIC method provides an effective practice for analyzing the direction and strength of cortical-muscular coupling. However, in cortical-muscular coupling, only a single EEG channel was analyzed, and the recorded signals represented a large number of superimposed signals from multiple oscillating sources. To address this limitation, TDBackMIC analysis of multi-channel EEG and EMG signals will be considered in future work. In addition, the sample size of this study was relatively small. Only N=10 subjects were recruited. However, based on a power analysis using published reports [25], [28], we estimated that a number of 10 subjects would be sufficient to detect the significance for the intended research. Future studies of larger samples are required to verify the findings of our preliminary findings.

VII. Conclusion

The TDBackMIC method proposed in this paper can accurately judge the causal relationship between variables and has stronger robustness on variable α than the TDMIC method. Further, the TDBackMIC method is applied to the analysis of functional cortical-muscular coupling and intermuscular coupling network under different grip forces. The experimental results show that with the increase of grip force, the strength of functional cortical-muscular coupling in beta frequency band decreases, the coupling relationship between muscles is closer

and the connectivity is better. TDBackMIC method provides an effective means for causal coupling analysis, and creates favorable conditions for in-depth study of motion control mechanism.

REFERENCES

[1] X. Xi et al., "Enhanced EEG-EMG coherence analysis based on hand movements," *Biomed. Signal Process. Control*, vol. 56, Feb. 2020, Art. no. 101727.

[2] S. H. Jang and J. P. Seo, "The distribution of the cortical origin of the corticoreticular pathway in the human brain: A diffusion tensor imaging study," *Somatosensory Motor Res.*, vol. 31, no. 4, pp. 204–208, Dec. 2014.

[3] B. A. Conway et al., "Synchronization between motor cortex and spinal motoneuronal pool during the performance of a maintained motor task in man," *J. Physiol.*, vol. 489, no. 3, pp. 917–924, Dec. 1995.

[4] W. Omlor, L. Patino, M.-C. Hepp-Reymond, and R. Kristeva, "Gamma-range corticomuscular coherence during dynamic force output," *NeuroImage*, vol. 34, no. 3, pp. 1191–1198, Feb. 2007.

[5] P. Xie et al., "A multidimensional visible evaluation model for stroke rehabilitation: A pilot study," *IEEE Trans. Neural Syst. Rehabil. Eng.*, vol. 31, pp. 1721–1731, 2023.

[6] R. Kenville et al., "Intermuscular coherence between homologous muscles during dynamic and static movement periods of bipedal squatting," *J. Neurophysiol.*, vol. 124, no. 4, pp. 1045–1055, Oct. 2020.

[7] X. Chen et al., "Multiscale information transfer in functional corticomuscular coupling estimation following stroke: A pilot study," *Frontiers Neurol.*, vol. 9, May 2018, Art. no. 00287.

[8] L.-J. Wang et al., "Muscle fatigue enhance beta band EMG-EMG coupling of antagonistic muscles in patients with post-stroke spasticity," *Frontiers Bioeng. Biotechnol.*, vol. 8, Aug. 2020, Art. no. 01007.

[9] Y. Gao, L. Ren, R. Li, and Y. Zhang, "Electroencephalogram–electromyography coupling analysis in stroke based on symbolic transfer entropy," *Frontiers Neurol.*, vol. 8, Jan. 2018, Art. no. 00716.

[10] J. T. Gwin and D. P. Ferris, "Beta- and gamma-range human lower limb corticomuscular coherence," *Frontiers Hum. Neurosci.*, vol. 6, Sep. 2012, Art. no. 00258.

[11] P. Madeleine, Y. Xie, G. P. Y. Szeto, and A. Samani, "Effects of chronic neck–shoulder pain on normalized mutual information analysis of surface electromyography during functional tasks," *Clin. Neurophysiol.*, vol. 127, no. 9, pp. 3110–3117, Sep. 2016.

[12] C. W. J. Granger, "Investigating causal relations by econometric models and cross-spectral methods," *Econometrica*, vol. 37, no. 3, pp. 424–438, Aug. 1969.

[13] T. Schreiber, "Measuring information transfer," *Phys. Rev. Lett.*, vol. 85, no. 2, pp. 461–464, Jul. 2000.

[14] X.-N. Zuo et al., "The oscillating brain: Complex and reliable," *NeuroImage*, vol. 49, no. 2, pp. 1432–1445, Jan. 2010.

[15] Q. She, H. Zheng, T. Tan, B. Zhang, Y. Fan, and Z. Luo, "Time-frequency-domain copula-based Granger causality and application to corticomuscular coupling in stroke," *Int. J. Humanoid Robot.*, vol. 16, no. 4, Aug. 2019, Art. no. 1950018.

[16] Z. Guo, V. M. McClelland, O. Simeone, K. R. Mills, and Z. Cvetkovic, "Multiscale wavelet transfer entropy with application to corticomuscular coupling analysis," *IEEE Trans. Biomed. Eng.*, vol. 69, no. 2, pp. 771–782, Feb. 2022.

[17] F. Ye, Z. Sun, D. Yang, H. Wang, and X. Xi, "Corticomuscular coupling analysis based on improved LSTM and transfer entropy," *Neurosci. Lett.*, vol. 760, no. 1, Aug. 2021, Art. no. 136012.

[18] S. Li, Y. Xiao, D. Zhou, and D. Cai, "Causal inference in nonlinear systems: Granger causality versus time-delayed mutual information," *Phys. Rev. E, Stat. Phys. Plasmas Fluids Relat. Interdiscip. Top.*, vol. 97, no. 5, May 2018, Art. no. 052216.

[19] D. N. Reshef et al., "Detecting novel associations in large data sets," *Science*, vol. 334, no. 6062, pp. 1518–1524, Dec. 2011.

[20] Y. Tian, H. Zhang, P. Li, and Y. Li, "A complementary method of PCC for the construction of scalp resting-state EEG connectome: Maximum information coefficient," *IEEE Access*, vol. 7, pp. 27146–27154, 2019.

[21] T. Liang, Q. Zhang, X. Liu, C. Lou, X. Liu, and H. Wang, "Time-frequency maximal information coefficient method and its application to functional corticomuscular coupling," *IEEE Trans. Neural Syst. Rehabil. Eng.*, vol. 28, no. 11, pp. 2515–2524, Nov. 2020.

[22] Y. Zhang, S. Jia, H. Huang, J. Qiu, and C. Zhou, "A novel algorithm for the precise calculation of the maximal information coefficient," *Sci. Rep.*, vol. 4, no. 1, pp. 1–5, Oct. 2014.

[23] Y. Chen, Y. Zeng, F. Luo, and Z. Yuan, "A new algorithm to optimize maximal information coefficient," *PLoS ONE*, vol. 11, no. 6, Jun. 2016, Art. no. e0157567.

[24] D. Cao, Y. Chen, J. Chen, H. Zhang, and Z. Yuan, "An improved algorithm for the maximal information coefficient and its application," *Roy. Soc. Open Sci.*, vol. 8, no. 2, Feb. 2021, Art. no. 201424.

[25] T. Liang et al., "Directed information flow analysis reveals muscle fatigue-related changes in muscle networks and corticomuscular coupling," *Frontiers Neurosci.*, vol. 15, Sep. 2021, Art. no. 750936.

[26] S. Zhu, J. Zhao, Y. Wu, and Q. She, "Intermuscular coupling network analysis of upper limbs based on R-vine copula transfer entropy," *Math. Biosciences Eng.*, vol. 19, no. 9, pp. 9437–9456, Jun. 2022.

[27] Q. Zhang, Y. Hu, T. Potter, R. Li, M. Quach, and Y. Zhang, "Establishing functional brain networks using a nonlinear partial directed coherence method to predict epileptic seizures," *J. Neurosci. Methods*, vol. 329, Jan. 2020, Art. no. 108447.

[28] V. Chakarov, J. R. Naranjo, J. Schulte-Mönting, W. Omlor, F. Huethe, and R. Kristeva, "Beta-range EEG-EMG coherence with isometric compensation for increasing modulated low-level forces," *J. Neurophysiol.*, vol. 102, no. 2, pp. 1115–1120, Aug. 2009.

[29] P. Xie et al., "Direct interaction on specific frequency bands in functional corticomuscular coupling," *IEEE Trans. Biomed. Eng.*, vol. 67, no. 3, pp. 762–772, Mar. 2020.

[30] J. Liu, G. Tan, Y. Sheng, and H. Liu, "Multiscale transfer spectral entropy for quantifying corticomuscular interaction," *IEEE J. Biomed. Health Informat.*, vol. 25, no. 6, pp. 2281–2292, Jun. 2021.

[31] T. Mima, T. Matsuoka, and M. Hallett, "Information flow from the sensorimotor cortex to muscle in humans," *Clin. Neurophysiol.*, vol. 112, no. 1, pp. 122–126, Jan. 2001.

[32] S. Mehrkanoon, M. Breakspear, and T. W. Boonstra, "The reorganization of corticomuscular coherence during a transition between sensorimotor states," *NeuroImage*, vol. 100, pp. 692–702, Oct. 2014.

[33] X. Chen, Y. Zhang, S. Cheng, and P. Xie, "Transfer spectral entropy and application to functional corticomuscular coupling," *IEEE Trans. Neural Syst. Rehabil. Eng.*, vol. 27, no. 5, pp. 1092–1102, May 2019.

[34] T. Gilbertson, E. Lalo, L. Doyle, V. Di Lazzaro, B. Cioni, and P. Brown, "Existing motor state is favored at the expense of new movement during 13–35 Hz oscillatory synchrony in the human corticospinal system," *J. Neurosci.*, vol. 25, no. 34, pp. 7771–7779, Aug. 2005.

[35] J. M. Kilner, S. N. Baker, S. Salenius, V. Jousmäki, R. Hari, and R. N. Lemon, "Task-dependent modulation of 15–30 Hz coherence between rectified EMGs from human hand and forearm muscles," *J. Physiol.*, vol. 516, no. 2, pp. 559–570, Sep. 2004.

[36] S. Kattla and M. M. Lowery, "Fatigue related changes in electromyographic coherence between synergistic hand muscles," *Exp. Brain Res.*, vol. 202, no. 1, pp. 89–99, Apr. 2010.